ACS APPLIED MATERIALS & INTERFACES

Research Article

www.acsami.org

Open-Circuit Voltage Enhancement on the Basis of Polymer Gel Electrolyte for a Highly Stable Dye-Sensitized Solar Cell

Congcong Wu,[†] Lichao Jia,[†] Siyao Guo,[†] Song Han,[‡] Bo Chi,*[,†] Jian Pu,[†] and Li Jian[†]

[†]Center for Fuel Cell Innovation, School of Materials Science and Engineering, Huazhong University of Science and Technology, Wuhan 430074, China

[‡]College of Forestry, Northeast Forestry University, Harbin 150040, China

ABSTRACT: Dye-sensitized solar cells (DSSC) have received considerable attention owing to their low preparation cost and easy fabrication process. However, one of the drawbacks that limits the further application of DSSC is their poor stability, arising from the leakage and volatilization of the liquid organic solvent in the electrolyte. Therefore, to improve the long-term stability of DSSC, polymer gel electrolyte was studied to replace the conventional liquid electrolyte in this work. The results show that compared to liquid electrolyte, DSSC with polymer gel electrolyte has a smaller short-circuit current (J_{sc}), which decreases with the increase of the polymer gelator. Nevertheless, with the employment of the polymer gel electrolyte, there is a significant enhancement of open-circuit voltage (V_{oc}), and it increases with the increase of the polymer gelator content. The highest V_{oc}, up to 0.873 V, can be obtained for DSSC with a 30% polymer gelator content. The impact of the polymer gel electrolyte on the photovoltaic performance of DSSC, especially on V_{oc}, was studied by analyzing the charge-transfer kinetics in the polymer gel electrolyte. Furthermore, the influence of the polymer gel electrolyte on the long-term stability of DSSC was also investigated.

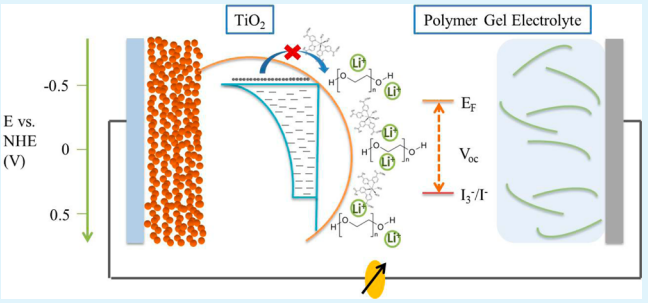

KEYWORDS: *polymer gel electrolyte, V_{oc} enhancement, mass transport, charge recombination, long-term stability*

1. INTRODUCTION

From the time that a dye-sensitized solar cell (DSSC) was demonstrated by O'Regan and Grätzel in 1991,[1,2] it has attracted considerable attention owing to its low production cost and easy fabrication procedure, providing a promising alternative to conventional silicon solar cells.[3] DSSC was constructed by a wide-band semiconductor mesoporous film sensitized by dye molecules. On photo excitation, the photo electrons are injected from excited dyes into the conducting band of the oxide semiconductor, and the oxidized dyes are regenerated by the redox couple in the electrolyte, whereas the hole in the electrolyte is reduced at the Pt counter electrode.[4] Although DSSCs have the potential to advance commercialization, there are some drawbacks that limit the commercial application of DSSCs. The most commonly used electrolyte in high-efficiency DSSCs is triiodide/iodide (I_3^-/I^-) dissolved in a volatile organic solvent.[5,6] However the leakage or volatilization of the liquid solvent in the electrolyte significantly deteriorates the long-term stability of the DSSCs. Thus, considerable efforts have been made to replace the liquid electrolyte with a solid-state electrolyte or quasi-solid-state electrolyte.[7−10] As a solid-state electrolyte, polymer electrolyte is usually formed by dissolving alkali metal salts into polymer matrix. However, the performance of a DSSC with polymer electrolyte is hampered by the low ionic diffusion in the polymer matrix.[11−13] Therefore, quasi-solid-state electrolyte, such as polymer gel electrolyte, formed by liquid electrolyte trapped in the polymer networks, has been suggested as the best choice for use in DSSCs. The polymer gel electrolyte combines the advantages of solid and liquid electrolytes, such as high stability and superior ionic diffusion, and can also facilitate the penetration of the electrolyte into the mesoporous TiO_2 film. It has been expected to be a promising candidate for the ideal electrolyte.[14,15]

From the time that a polymer gel electrolyte was reported to be applied in electrochemical devices, it has received extensive investigation. Various modifications of polymer systems were carried out to improve the performance of the polymer gel electrolyte. Compounds such as crown ether molecules, *t*-bromomethylbenzene, and γ-butyrolactone have become common additives to elaborate polymer gel electrolyte.[16−18] Recently, owing to the unique property of room-temperature ionic liquids (RTIL), polymer gel electrolytes incorporating various RTIL were also attempted.[19−23] Other investigations of polymer gel electrolyte were focused on the nanostructure fillings into the electrolyte, such as SiO_2, TiO_2 nanoparticles, carbon nanotubes, and so on.[24−27] Despite the fact that a comparable performance of these polymer gel electrolytes has been achieved, DSSCs with polymer gel electrolyte still show a lower efficiency compared to those with liquid electrolyte. One

Received: May 24, 2013
Accepted: July 30, 2013
Published: July 30, 2013

of the main reasons is the insufficient understanding of the charge-transfer kinetics in the polymer gel electrolyte. Many studies are emphasizing the effect of the additives, whereas the role of the gelator in the interfacial charge transfer is always neglected. Here, in this research, we show an enhancement of the open-circuit voltage (V_{oc}) of a DSSC upon the employment of polymer gel electrolyte, and we further analyze the charge-transfer process in the polymer gel electrolyte to reveal the origin of the influence of the gelator on the photovoltaic performance of the DSSC.

Poly(ethylene oxide) (PEO) has been the most commonly used polymer matrix to prepare polymer electrolyte because of its excellent chemical stability and high ionic dissociation.[28,29] Therefore, in this work, we applied PEO to solidify the liquid phase for preparing polymer gel electrolytes. In contrast to the liquid electrolyte, the ionic-transport characteristics of polymer gel electrolyte were investigated. Of particular interest in this work, we focused on the dependence of the polymer gelator content on the V_{oc} of the DSSC, and we discovered the origin of the increased V_{oc} with the employment of polymer gel electrolyte by analyzing the impact of the polymer gel electrolyte on the kinetics of charge transfer at the TiO_2/electrolyte interface. Furthermore, the charge transfer at the Pt counter electrode was investigated, and we give a detailed explanation of the electrochemical processes in the polymer gel electrolyte. In addition, the long-term stability of the DSSCs using polymer gel electrolyte was tested, and the effect of gelator on the durability was analyzed.

2. EXPERIMENTAL SECTION

2.1. Materials and Electrolytes Preparation. PEO (MW 100 000), LiI (ultra dry, 99 wt %), ethylene carbonate (EC), and propylene carbonate (PC) were purchased from Alfa Aesar. I_2 was provided by Shanghai Experiment Reagent Co. Ltd. 4-*tert*-butylpyridine (4-TBP) was supplied by Sigma-Aldrich. N719 dye was purchased from Solaronix (Switzerland). Acetonitrile, *tert*-butanol, terpinol, and ethyl cellulose were from Sinopharm Chemical Reagent Co. Ltd. FTO conducting glasses (14 Ω sq^{-1}) were provided by Nippon Sheet Glass Co. Ltd. (Japan), and H_2PtCl_6 was supplied by Chameleon Reagent.

First, the liquid electrolyte was prepared by adding the predetermined amount of LiI (0.5 M), I_2 (0.05 M), and 4-TBP (0.5 M) into the organic solvent containing EC and PC with a volume ratio of 1:1. The resulting mixture was stirred until no solids were observed. Polymer gel electrolytes were prepared by dissolving different amounts of the polymer gelator (PEO) into the liquid electrolyte, with the content of the gelator at 10, 15, 20, 25, and 30 wt %. The mixture was stirred for 12 h to completely dissolve the PEO and was kept in air conditioned at room temperature for 72 h for the polymerization.

2.2. DSSC Fabrication. TiO_2 paste was prepared by mixing 25 wt % P25 power (Degussa) with 75 wt % terpinol containing ethyl cellulose. The TiO_2 film electrode was prepared by screen printing the TiO_2 paste on the FTO glass followed by sintering at 450 °C for 1 h and cooling to room temperature. The TiO_2 film electrode was sensitized by immersion into a 0.3 mM solution of N719 dye in acetonitrile and *tert*-butanol (volume ratio 1:1) at room temperature for 12 h. The Pt counter electrode was prepared by spreading a 10 mM solution of H_2PtCl_6 in terpinol on FTO glass, which was heated at 450 °C for 1 h. Finally, the DSSCs were fabricated by the assembly of the photoanode and counter electrode with thermoplastic film (Surlyn, Dupont), and the internal spacer between the electrodes was filled with the prepared electrolyte.

2.3. Electrochemical Characterization. A solar simulator with a 300 W xenon lamp (91160, Newport) was used to give 1 sun illumination (AM 1.5, 100 mW cm^{-2}). All of the electrochemical measurements were carried out with an electrochemical workstation (Zennium, Zahner). The current–voltage characteristics were measured by applying a potential sweep to DSSC, and the generated photocurrent was recorded as the potential sweep. Electrochemical impedance spectroscopy (EIS) was measured in 1 sun illumination in an open-circuit and in the dark, with a forward bias from 0.5 to 0.7 V and with a frequency range from 10^5 to 10^{-1} Hz at an amplitude of 10 mV. The obtained spectra were fitted by Zview software (Scribner Associates Inc.). The temperature dependence of the onic conductivity was determined from the EIS measurements from 30 to 70 °C. The polymer gel electrolytes were sandwiched in the Teflon ring gap between two stainless steel electrodes, and the ionic conductivity was calculated by the equation $\sigma = L/AR_b$, where L is the thickness of the polymer gel electrolyte, A is the surface area of the polymer gel electrolyte, and R_b is the bulk resistance of the polymer gel electrolyte. The mass transport characteristics of the electrolytes were investigated by measuring the linear sweep voltammetry of the symmetrical dummy cell from −1.5 to 1.5 V. The dummy cell is composed of two identical Pt electrodes, with the electrolyte filled in the space gap between the two electrodes.

3. RESULTS AND DISCUSSION

3.1. Photovoltaic Performance. Figure 1 shows the current–voltage characteristics of the DSSCs employing liquid and polymer gel electrolytes measured at 1 sun illumination. The liquid electrolyte shows an open-circuit voltage (V_{oc}) of 0.775 V, a short-circuit current density (J_{sc}) of 9.14 mA cm^{-2}, and a fill factor (FF) of 0.60, corresponding to a power conversion efficiency (PCE) of 4.2%. The details of the photovoltaic parameter summaries are listed in Table 1. It was observed that the application of polymer gel electrolyte results in an obvious enhancement of V_{oc} compared with that of the liquid electrolyte. The polymer gel electrolyte with 10% gelator

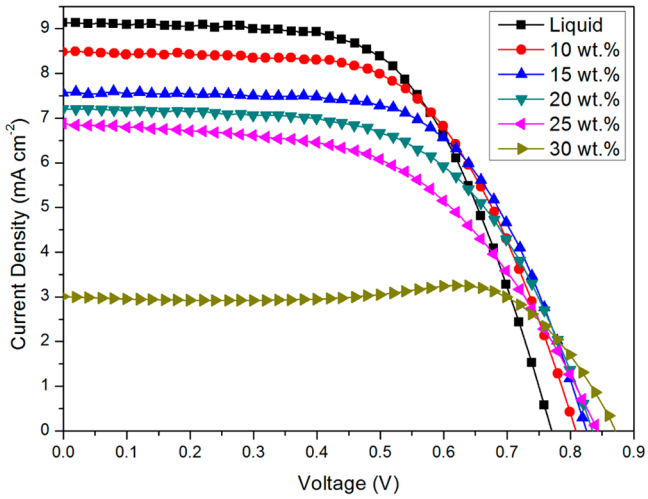

Figure 1. Current–voltage characteristics of the DSSCs employing liquid electrolyte and polymer gel electrolytes with different gelator content.

Table 1. Photovoltaic Parameters for the DSSCs Employing Liquid Electrolyte and Polymer Gel Electrolytes

electrolyte (wt %)	V_{oc} (V)	J_{sc} (mA cm^{-2})	FF	η (%)
0	0.775	9.14	0.60	4.2
10	0.810	8.46	0.60	4.1
15	0.825	7.54	0.63	3.9
20	0.832	7.22	0.60	3.6
25	0.842	6.86	0.54	3.1
30	0.873	3.03	0.79	2.1

dx.doi.org/10.1021/am4019548 | ACS Appl. Mater. Interfaces 2013, 5, 7886–7892

exhibits a V_{oc} value of 0.810 V. Furthermore, the change in the increment of gelator content leads to the gradual increase of V_{oc}, and the highest V_{oc} value of 0.873 V is obtained for 30% polymer gel electrolyte, which is approximately 100 mV higher than that of the liquid electrolyte. However, the tendency of J_{sc} is minimally different. The liquid electrolyte has the highest J_{sc} owing to the superior ionic diffusion characteristics of the liquid solvent. The J_{sc} of polymer gel electrolytes are lower than that of liquid electrolyte, and they decrease with the increase of gelator content. In addition, when the gelator content increases to 30%, J_{sc} of DSSC decreases rapidly to 3.03 mA cm^{-2}. The decreased J_{sc} results from the slower ionic diffusion that occurs with the introduction of the polymer gelator. Moreover, when an excessive amount of gelator is introduced, the polymer gel electrolyte is dominated by the crystalline polymer matrix, which shows inferior ionic-transport performance and leads to the decreases of J_{sc}.

3.2. Mass Transport in the Polymer Gel Electrolyte. To clarify the dependence of J_{sc} on the composition of the electrolytes, the mass transport characteristics of the electrolytes were investigated. Figure 2 shows the linear sweep

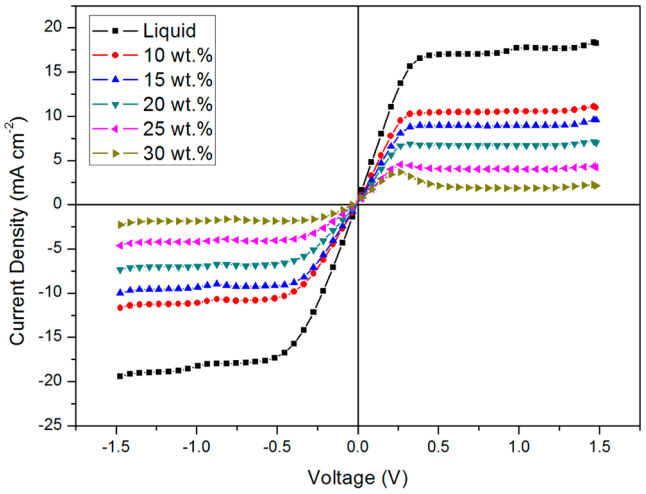

Figure 2. Linear sweep voltammetry of symmetrical dummy cells employing liquid electrolyte and polymer gel electrolytes with different gelator content.

voltammetry of symmetrical dummy cells employing liquid electrolyte and various polymer gel electrolytes. All of the curves exhibit the platform of limiting current (J_{lim}), which is determined by the diffusion of the charge carriers in the electrolyte. The liquid electrolyte yields the largest J_{lim}; however, the polymer gel electrolytes show a significant decrease in J_{lim}. In addition, J_{lim} of the polymer gel electrolyte decreases with the increase of the gelator content, which is in agreement with J_{sc} of DSSC, confirming that the limited ionic-diffusion flux leads to the lower J_{sc} of the polymer gel electrolytes. From J_{lim}, we can calculate the diffusion coefficient of triiodide according to the equation $J_{lim} = 2nFCD/L$, where n is the number of electrons transferred in the electrode reaction, F is the Faraday constant, C is the bulk concentration of triiodide, D is the diffusion coefficient, and L is the thickness of the spacer.[30,31] The diffusion coefficient of triiodide for liquid electrolyte is 4.58×10^{-6} cm^2 s^{-1}, whereas it is 2.73×10^{-6}, 2.32×10^{-6}, 1.83×10^{-6}, 1.13×10^{-6}, and 6.00×10^{-7} cm^2 s^{-1} for the polymer gel electrolytes with gelator content increasing from 10% to 30%, respectively. The diffusion coefficient of triiodide in the liquid electrolyte is several times larger than that for the polymer gel electrolyte, and it decreases with the increase of the gelator content in polymer gel electrolyte. The result suggests that the diffusion of triiodide in polymer gel electrolyte is retarded by the polymer gelator.

To obtain further insight into the ionic-transport behavior in the polymer gel electrolyte, ionic conductivity was measured. Figure 3 shows the plots of the ionic conductivity against $1/T$

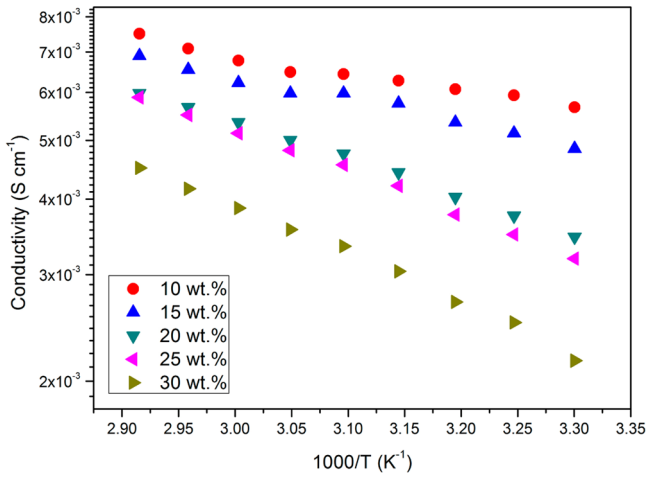

Figure 3. Temperature dependence of the ionic conductivity in polymer gel electrolytes with different gelator content.

for the polymer gel electrolytes, and the temperature dependence exhibits an Arrehenius behavior that can be fitted with the equation $\sigma = \sigma_0 \exp(-E_A/kT)$, where σ is the ionic conductivity, E_A is the activation energy, and k is Boltzmann's constant. It is shown that the ionic conductivity decreases with the increase of gelator content, confirming that the ionic transport is suppressed by the gelator in the polymer gel electrolyte. Furthermore, the activation energy of the polymer gel electrolyte also increases with the gelator content, which is 5.47, 7.15, 11.88, 13.19, and 15.41 kJ mol^{-1}, respectively. The results indicate that the charge-transport behavior is influenced by the polymer gelator, which is in agreement with the result of the diffusion coefficient of triiodide. In the polymer gel electrolyte, the 3D polymer matrix holds the liquid solution via cross links.[32,33] With the changing increment of the polymer gelator, the cross links between the polymer gelator and the liquid solvent reduce the ionic-transport channel and thus hinder the physical diffusion of the ions, which results in the increase of the activation energy with the increase in the gelator content.[34] The results explain the decreased J_{sc} with the increment of polymer gelator.

3.3. Origin of the Voltage Enhancement for the Polymer Gel Electrolyte. The electrolyte has an apparent influence on DSSC photovoltaic performance by affecting the charge-carrier transfer kinetics. From the current−voltage characteristics of DSSCs, it was observed that there is a significant improvement of V_{oc} upon the employment of polymer gel electrolyte.

The measured V_{oc} is defined as the potential different between the quasi-Fermi level of the electrons in TiO_2 under illumination and the redox potential of the redox couple in the electrolyte, which can be expressed as

$$qV_{oc} = E_F - E_{redox} \quad (1)$$

The quasi-Fermi level of the electron in TiO_2 is given by

$$E_F = E_C + kT \ln \frac{n_c}{N_C} \quad (2)$$

Thus, V_{oc} is determined by

$$V_{oc} = \frac{kT}{q}\left(\frac{E_C - E_{redox}}{kT} + \ln \frac{n_c}{N_C}\right) \quad (3)$$

where E_F is the quasi-Fermi level of the electron in TiO_2, E_{redox} is the redox potential of the redox couple, E_C is the conduction band edge of TiO_2, kT is the thermal energy, n_c is the free electron density in the conduction band of TiO_2, and N_C is the density of the accessible state in the conduction band. Therefore, it is noted that both the negative shift of the conduction band edge of TiO_2 (E_C) and the higher density of the free electron in the conduction band (n_c) of TiO_2 will give rise to an increase in V_{oc}. However, n_c is determined by the electron recombination rate at a given flux of illumination. Hence, we can associate the enhancement of V_{oc} with the shift of the E_C band edge and the interfacial charge recombination kinetics at the TiO_2/electrolyte interface.

To determine the influence of the polymer gel electrolyte on the conduction band edge of TiO_2, we carried out EIS measurements on the electrolytes under dark conditions at different bias. Figure 4 presents the effect of the applied voltage

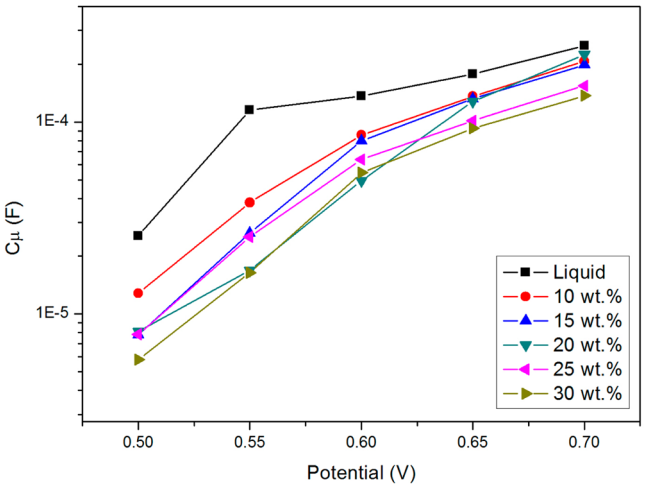

Figure 4. Chemical capacitance, C_μ, as a function of applied bias obtained from EIS under dark conditions.

on the chemical capacitance C_μ for the electrolytes. The applied bias represents the potential differences between the quasi-Fermi level of TiO_2 and the redox potential of electrolyte. C_μ reflects the accumulated electron density with the variation of applied potential, which provides a quantitative estimation of the E_C band edge of TiO_2. The capacitance, C_μ, can be expressed as[35,36]

$$C_\mu = L(1-p)\,\alpha \frac{q^2 N_L}{kT} \exp[\alpha(E_{redox} - E_C)/kT] \quad (4)$$

where L is the TiO_2 film thickness, p is the porosity, and N_L is the density of trap states below the E_c of TiO_2. From eq 4, it was observed that, provided the identical geometrical dimensions of the TiO_2 photoanode, the variation of the capacitance is equivalent to the shift of the E_C band edge. As shown in Figure 4, at a given capacitance the bias potential for the polymer gel electrolyte is higher than that of the liquid electrolyte, indicating the negative shift of the E_C band edge of TiO_2 of the polymer gel electrolytes, which contributes to the increase of V_{oc} upon the introduction of the polymer gel electrolyte.

To clarify the impacts of the polymer gel electrolyte on the interfacial charge-transfer processes, we carried out the measurement of the dark-current characteristics of DSSCs with different electrolytes. Under dark conditions with forward bias, the electrons are injected from the FTO glass into the conduction band of TiO_2 and then travel through the mesoporous TiO_2 film, where they are captured by the triiodide in the electrolyte. The dark current indicates the kinetics of the reaction of the injected electrons with triiodide in the electrolyte. It was observed that under the same bias, the liquid electrolyte has the largest dark current, indicating that the liquid electrolyte has a larger recombination kinetic constant compared with the polymer gel electrolyte, as shown in Figure 5. In addition, the dark current decreases with the increase of

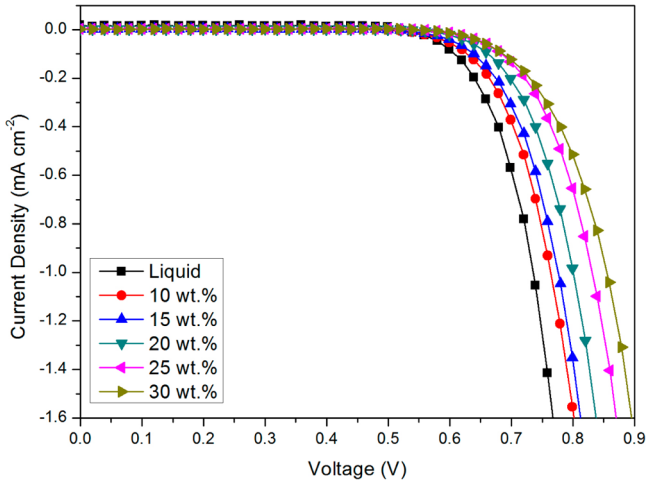

Figure 5. Current−voltage characteristics of the DSSCs employing liquid electrolyte and polymer gel electrolytes with different gelator content under dark conditions.

gelator content, suggesting that the polymer gel electrolyte can suppress the reaction of the injected electrons with the triiodide in the electrolyte, and the recombination rate decreases with the increment of the polymer gelator.

To clarify further the effect of the polymer gel electrolyte on the interfacial charge-transfer processes, EIS under 1 sun illumination at open circuit was performed. The EIS under illumination exhibits three semicircles, as shown in Figure 6. The high-frequency range represents the charge transfer at the Pt counter electrode ($R_{ct,pt}$), the middle-frequency range is related to the charge transport (R_t)/recombination (R_{ct}) at the TiO_2/electrolyte interface, and the low-frequency range is assigned to the ionic diffusion in the electrolyte. The EIS can be fitted with an equivalent circuit on the basis of the transmission line model.[37,38] To elucidate the interfacial charge-transfer processes, here we focus on the middle-frequency semicircle. The fitted charge-recombination resistance, R_{ct}, is shown in Figure 7. The R_{ct} of the polymer gel electrolyte increases compared with that of the liquid electrolyte. Moreover, it increases with the increment of the gelator content. The increased R_{ct} represents the suppression of the charge recombination at the TiO_2/electrolyte interface. Furthermore,

dx.doi.org/10.1021/am4019548 | ACS Appl. Mater. Interfaces 2013, 5, 7886−7892

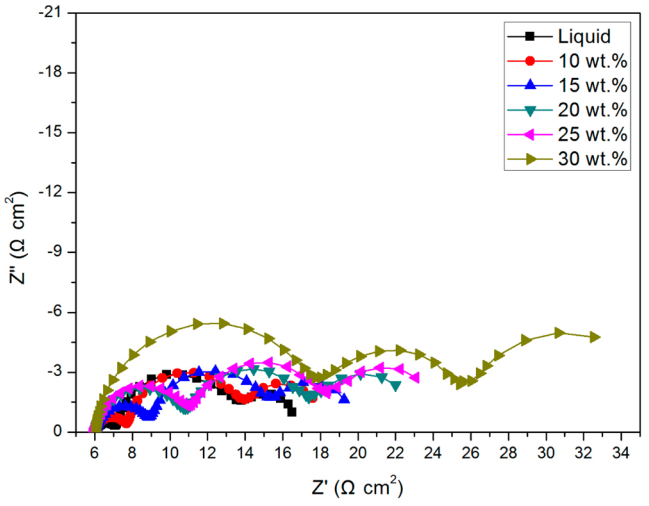

Figure 6. EIS of the DSSCs employing liquid electrolyte and polymer gel electrolytes with different gelator content obtained under AM 1.5 illumination at open circuit.

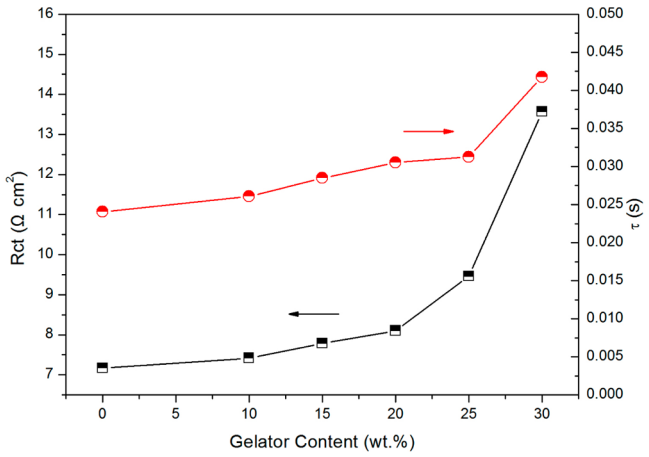

Figure 7. Charge recombination resistance, R_{ct}, and electron lifetime, τ_n, versus polymer gelator content.

the electron lifetime, τ_n, which can be calculated from the equation $\tau_n = R_{ct}C_\mu$, also increases with the increase of gelator content, as shown in Figure 7, implying that the electron recombination is retarded with the employment of the polymer gel electrolyte, which is consistent with the dark-current characteristics.

From the above results, we can conclude that the improvement of V_{oc} originates from the negative shift of the E_C band edge of TiO_2 and the suppression of electron recombination at the TiO_2/electrolyte interface. It is assumed that when the electrons are injected into the conduction band of TiO_2 from the dye sensitizer the Li^+ cations are likely to be absorbed on the negative charged TiO_2 particle, forming the electric double layer (Helmholtz layer) at the TiO_2 particle surface. The potential drop in the Helmholtz layer, therefore, gives a positive shift of the E_C band edge of TiO_2.[39−42] However, in the polymer gel electrolyte, PEO is used as the gelator, and the ether oxygens in the polymer chain are considered to be hard bases, which will form complex with hard Li^+ cations.[43,44] Therefore, the Li^+ cations are coordinated with the PEO chain, correspondingly decreasing the amount of the absorbed Li^+ on the surface of TiO_2 particle and thereby resulting in the shift of the E_C band edge back to a negative position, as shown in Scheme 1. Furthermore, with the

Scheme 1. Illustrations of the Surface States and Energy Bands at the TiO_2/Electrolyte Interface in the DSSC Employing Liquid Electrolyte and Polymer Gel Electrolyte

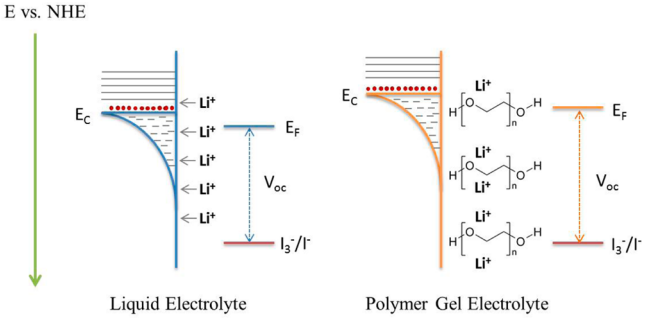

employment of the polymer gel electrolyte, the gelator of PEO is coated on the surface of the TiO_2 particle as a passivation layer, blocking the charge recombination between the electrons in TiO_2 and triiodide in the electrolyte, which results in the decreased recombination and increased electron lifetime of the polymer gel electrolytes.

Figure 8 shows the electron transport resistance, R_t, and electron diffusion coefficient, D_e, of the electrolytes obtained by

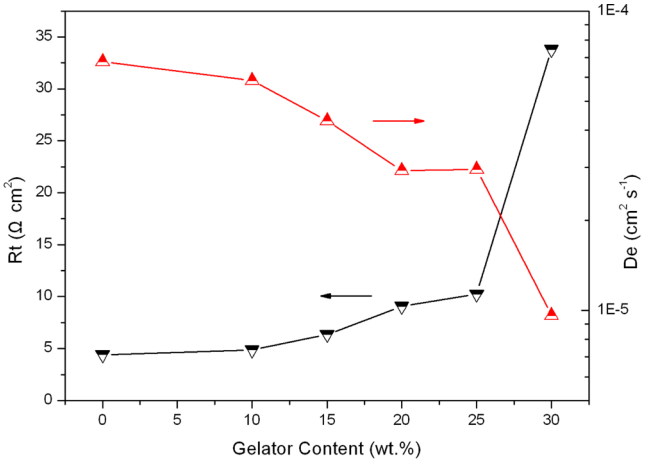

Figure 8. Charge transport resistance, R_t, and electron diffusion coefficient, D_e, versus polymer gelator content.

fitting EIS with the equivalent circuit. The fitted parameters are listed in Table 2. R_t increases and D_e decreases with the increasing of the gelator content. The results can be also explained by the theoretical model discussed above. It is assumed that the electron diffusion coefficient, D_e, in the mesoporous TiO_2 film is influenced by the absorbed Li^+ cations. The value of D_e increases with the increasing Li^+ concentration, which is attributed to the effect of an ambipolar diffusion mechanism.[45−47] However, as the gelator content increases, the concentration of Li^+ decreases by the coordination of Li^+ with PEO chain, leading to the decrease of diffusion coefficient D_e.[48] The results provide further evidence for the effect of polymer gelator in the polymer gel electrolyte, which serves as the passivation layer on surface of TiO_2, with Li^+ trapped in the ether oxygen units in the polymer gelator. The role of the polymer gelator in the interfacial

dx.doi.org/10.1021/am4019548 | ACS Appl. Mater. Interfaces 2013, 5, 7886−7892

Table 2. Electron Transport Resistance, R_t, and Electron Diffusion Coefficient, D_e, of the DSSCs with Liquid Electrolyte and Polymer Gel Electrolytes

electrolyte	0 wt %	10 wt %	15 wt %	20 wt %	25 wt %	30 wt %
R_t (Ω cm^2)	4.40	4.86	6.36	9.06	10.24	33.79
D_e (cm^2 s^{-1})	6.77×10^{-5}	5.85×10^{-5}	4.30×10^{-5}	2.93×10^{-5}	2.95×10^{-5}	9.61×10^{-6}

interaction leads to the negative shift of the E_C band edge and reduces the charge recombination, resulting in the enhancement of V_{oc} with the polymer gel electrolyte.

3.4. Charge Transfer at the Pt Counter Electrode. From the EIS measurements under illumination, as shown in Figure 6, it is should be noted that there are apparent differences in the charge-transfer resistance, $R_{ct,Pt}$, at the Pt counter electrolyte. It has been confirmed that $R_{ct,Pt}$ increases with the increment of the gelator content (Figure 6). The $R_{ct,Pt}$ value for the liquid electrolyte is 1.21 Ω cm^2, whereas the R_{ct} values for the polymer gel electrolyte with gelator content of 10, 15, 20, 25 and 30% are 1.78, 3.14, 5.29, 5.53, and 12.49 Ω cm^2, respectively. Strikingly, the $R_{ct,Pt}$ value of the 30% polymer gel electrolyte is about 10 times larger than that of the liquid electrolyte. At the Pt counter electrode, the electrons from the external circle are transferred to the electrolyte through the charge-transfer reaction between triiodide and iodide. Thus, $R_{ct,Pt}$ indicates the performance of triiodide reduction at the Pt counter electrode, which is influenced by the charge-transfer process at the Pt counter electrode/electrolyte interface and the ion concentration at the surface of counter electrode. Therefore, the increased $R_{ct,Pt}$ in the polymer gel electrolyte implies that the polymer gelator interferes the charge transfer at the counter electrode. This is mainly attributed to the adsorption of the gelator on the Pt counter electrode, which prevents the contact of triiodide with the Pt counter electrode. Furthermore, owing to the lower ionic diffusion in the polymer gel electrolyte, the deviation of the surface concentrations of triiodide also contributes to the large $R_{ct,Pt}$ in the polymer gel electrolyte.[49] The results suggest that the DSSCs with polymer gel electrolyte can be further optimized by developing a more suitable counter electrode for the polymer gel electrolyte.

3.5. Long-Term Stability of the Cells. The long-term stability of DSSCs with liquid and polymer gel electrolytes was investigated with a duration of 1100 h in air at room temperature, and the results are shown in Figure 9. The J_{sc} value of DSSCs with liquid electrolyte decays sharply by 200 h (Figure 9a). The performance degradation is mainly because of the solvent volatilization of the liquid electrolyte. When polymer electrolytes are employed, the stability performance is greatly improved. After 200 h of testing, J_{sc} for DSSC with polymer gel electrolyte moderately increases. After 1100 h of testing, the J_{sc} values for DSSC with polymer electrolytes of 10 and 15% gelator decrease sharply and remain at only 20 and 25% of the initial performance, which mainly arises from the solvent permeation across the sealing film between the electrodes. With the gelator content increasing, an improvement in the stability can be observed. The J_{sc} values for DSSC with 20, 25, and 30% gelator remain at 75, 92, and 100% of their initial values, respectively. No degradation is observed for DSSC with 30% gelator even after 1100 h testing, whereas the V_{oc} values of these DSSCs with different electrolytes remain almost constant (Figure 9b). The results imply that the polymer gel electrolyte can suppress the leakage or volatilization of solvent, improving the durability and reliability of the device. It can be concluded, therefore, that the polymer

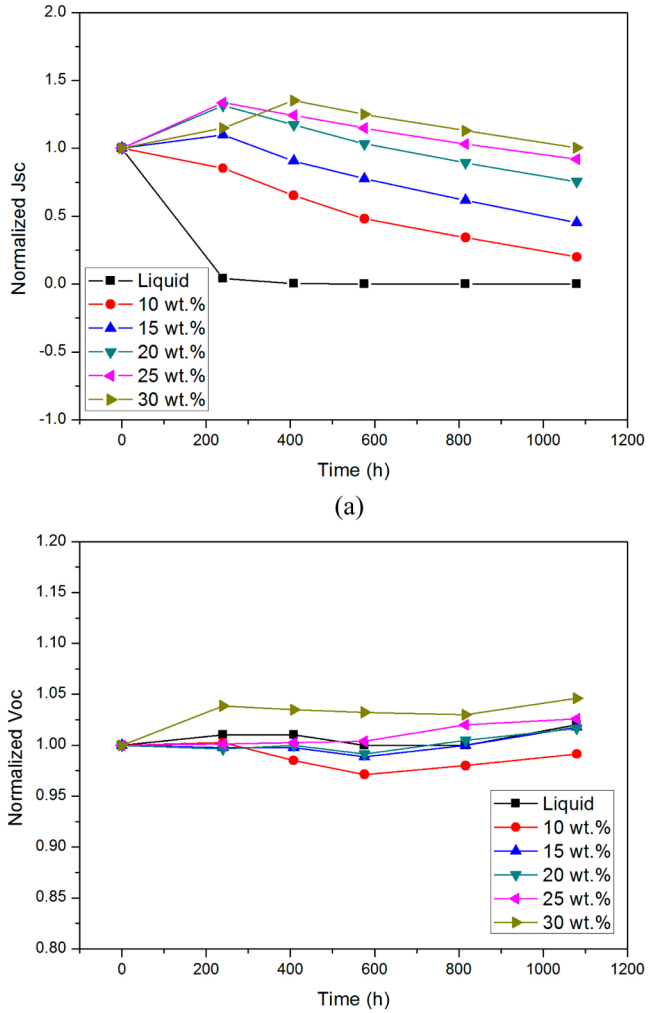

Figure 9. Normalized J_{sc} (a) and V_{oc} (b) values of the DSSCs employing liquid electrolyte and polymer gel electrolytes with different gelator content during 1100 h of testing.

gel electrolyte plays a dual role in DSSC, modulating the interfacial charge-transfer kinetics for the enhancement of V_{oc} and improving the long-term stability of the DSSC. The implications of this research give a direction for the pursuit of a high-performance DSSC with further improved stability.

4. CONCLUSIONS

In this article, the enhancement of V_{oc} and the long-term stability of DSSC were studied using polymer gel electrolyte. On the basis of the results and the analysis of the study, the following conclusions can be made: (1) The employment of polymer gel electrolyte can significantly enhance V_{oc}. The DSSC with the highest V_{oc} of 0.873 V was obtained for the polymer gel electrolyte with 30% gelator; (2) the analysis confirms that the negative shift of the conduction band edge of

dx.doi.org/10.1021/am4019548 | ACS Appl. Mater. Interfaces 2013, 5, 7886−7892

TiO_2 and the suppression of charge recombination at the TiO_2/electrolyte interface in DSSCs with polymer gel electrolyte are considered to be the major factors leading to the improvement of V_{oc}; (3) the addition of the polymer gelator would decrease the J_{sc} of the DSSC because of the slow ionic diffusion in the polymer gel electrolyte together with the limitation of the mass transport in the electrolyte and the charge transfer at the Pt counter electrode; and (4) DSSCs with polymer gel electrolyte exhibit excellent durability and stability compared to that with liquid electrolyte. After 1100 h of testing, no performance degradation was observed for the DSSC with polymer gel electrolyte of 30% gelator.

AUTHOR INFORMATION

Corresponding Author

*E-mail: chibo@hust.edu.cn; Tel/Fax: +86-27-87558142.

Notes

The authors declare no competing financial interest.

ACKNOWLEDGMENTS

This research is financially supported by the National Natural Science Foundation of China (50902056). The authors thank the Materials Characterization Center of the Huazhong University of Science and Technology for samples measurement assistance.

REFERENCES

(1) O'Regan, B.; Grätzel, M. *Nature* **1991**, *353*, 737−740.
(2) Bach, U.; Lupo, D.; Comte, P.; Moser, J. E.; Weissortel, F.; Salbeck, J.; Spreitzer, H.; Grätzel, M. *Nature* **1998**, *395*, 583−585.
(3) Grätzel, M. *Nature* **2001**, *414*, 338−344.
(4) Grätzel, M. *Prog. Photovoltaics* **2000**, *8*, 171−185.
(5) Nasr, C.; Hotchandani, S.; Kamat, P. V. *J. Phys. Chem. B* **1998**, *102*, 4944−4951.
(6) Kebede, Z.; Lindquist, S.-E. *Sol. Energy Mater. Sol. Cells* **1999**, *57*, 259−275.
(7) Ren, Y.; Zhang, Z.; Fang, S.; Yang, M.; Cai, S. *Sol. Energy Mater. Sol. Cells* **2002**, *71*, 253−259.
(8) Nogueira, A. F.; Durrant, J. R.; De Paoli, M. A. *Adv. Mater.* **2001**, *13*, 826−830.
(9) Yoon, J.; Kang, D. K.; Won, J.; Park, J.-Y.; Kang, Y. S. *J. Power Sources* **2012**, *201*, 395−401.
(10) Chung, I.; Lee, B.; He, J.; Chang, R. P. H.; Kanatzidis, M. G. *Nature* **2012**, *485*, 486−489.
(11) Armand, M. *Adv. Mater.* **1990**, *2*, 278−286.
(12) Zhang, C.; Gamble, S.; Ainsworth, D.; Slawin, A. M. Z.; Andreev, Y. G.; Bruce, P. G. *Nat. Mater.* **2009**, *8*, 580−584.
(13) Nogueira, A. F.; De Paoli, M.-A.; Montanari, I.; Monkhouse, R.; Nelson, J.; Durrant, J. R. *J. Phys. Chem. B* **2001**, *105*, 7517−7524.
(14) Song, J. Y.; Wang, Y. Y.; Wan, C. C. *J. Power Sources* **1999**, *77*, 183−197.
(15) Cao, F.; Oskam, G.; Searson, P. C. *J. Phys. Chem.* **1995**, *99*, 17071−17073.
(16) Benedetti, J. E.; De Paoli, M. A.; Nogueira, A. F. *Chem. Commun.* **2008**, *0*, 1121−1123.
(17) Kato, T.; Fujimoto, M.; Kado, T.; Sakaguchi, S.; Kosugi, D.; Shiratuchi, R.; Takashima, W.; Kaneto, K.; Hayase, S. *J. Electrochem. Soc.* **2005**, *152*, A1105−A1108.
(18) Mikoshiba, S.; Murai, S.; Sumino, H.; Hayase, S. *Chem. Lett.* **2002**, *31*, 918−919.
(19) Wang, P.; Zakeeruddin, S. M.; Exnar, I.; Grätzel, M. *Chem. Commun.* **2002**, *0*, 2972−2973.
(20) Freitas, F. S.; de Freitas, J. N.; Ito, B. I.; De Paoli, M.-A.; Nogueira, A. F. *ACS Appl. Mater. Interfaces* **2009**, *1*, 2870−2877.
(21) Lu, J.; Yan, F.; Texter, J. *Prog. Polym. Sci.* **2009**, *34*, 431−448.
(22) Kubo, W.; Kambe, S.; Nakade, S.; Kitamura, T.; Hanabusa, K.; Wada, Y.; Yanagida, S. *J. Phys. Chem. B* **2003**, *107*, 4374−4381.
(23) Stergiopoulos, T.; Rozi, E.; Hahn, R.; Schmuki, P.; Falaras, P. *Adv. Energy Mater.* **2011**, *1*, 569−572.
(24) Bai, S.; Bu, C.; Tai, Q.; Liang, L.; Liu, Y.; You, S.; Yu, Z.; Guo, S.; Zhao, X. *ACS Appl. Mater. Interfaces* **2013**, *5*, 3356−3361.
(25) Huo, Z.; Dai, S.; Wang, K.; Kong, F.; Zhang, C.; Pan, X.; Fang, X. *Sol. Energy Mater. Sol. Cells* **2007**, *91*, 1959−1965.
(26) Usui, H.; Matsui, H.; Tanabe, N.; Yanagida, S. *J. Photochem. Photobiol., A* **2004**, *164*, 97−101.
(27) Wang, P.; Zakeeruddin, S. M.; Grätzel, M. *J. Fluorine Chem.* **2004**, *125*, 1241−1245.
(28) Armand, M. *Solid State Ionics* **1994**, *69*, 309−319.
(29) Bruce, P. G.; Vincent, C. A. *J. Chem. Soc., Faraday Trans.* **1993**, *89*, 3187−3203.
(30) Hauch, A.; Georg, A. *Electrochim. Acta* **2001**, *46*, 3457−3466.
(31) Papageorgiou, N.; Athanassov, Y.; Armand, M.; Bonhote, P.; Pettersson, H.; Azam, A.; Grätzel, M. *J. Electrochem. Soc.* **1996**, *143*, 3099−3108.
(32) Nogueira, A. F.; Longo, C.; De Paoli, M.-A. *Coord. Chem. Rev.* **2004**, *248*, 1455−1468.
(33) De Freitas, J. N.; Nogueira, A. F.; De Paoli, M.-A. *J. Mater. Chem.* **2009**, *19*, 5279−5294.
(34) Huo, Z.; Dai, S.; Zhang, C.; Kong, F.; Fang, X.; Guo, L.; Liu, W.; Hu, L.; Pan, X.; Wang, K. *J. Phys. Chem. B* **2008**, *112*, 12927−33.
(35) Barea, E. M.; Ortiz, J.; Paya, F. J.; Fernandez-Lazaro, F.; Fabregat-Santiago, F.; Sastre-Santos, A.; Bisquert, J. *Energy Environ. Sci.* **2010**, *3*, 1985−1994.
(36) Bisquert, J. *Phys. Chem. Chem. Phys.* **2003**, *5*, 5360−5364.
(37) Bisquert, J.; Grätzel, M.; Wang, Q.; Fabregat-Santiago, F. *J. Phys. Chem. B* **2006**, *110*, 11284−11290.
(38) Bisquert, J. *J. Phys. Chem. B* **2001**, *106*, 325−333.
(39) Cahen, D.; Hodes, G.; Grätzel, M.; Guillemoles, J. F.; Riess, I. *J. Phys. Chem. B* **2000**, *104*, 2053−2059.
(40) Liu, Y.; Hagfeldt, A.; Xiao, X.-R.; Lindquist, S.-E. *Sol. Energy Mater. Sol. Cells* **1998**, *55*, 267−281.
(41) Lyon, L. A.; Hupp, J. T. *J. Phys. Chem.* **1995**, *99*, 15718−15720.
(42) Redmond, G.; Fitzmaurice, D. *J. Phys. Chem.* **1993**, *97*, 1426−1430.
(43) Armand, M. *Adv. Mater.* **1990**, *2*, 278−286.
(44) MacGlashan, G. S.; Andreev, Y. G.; Bruce, P. G. *Nature* **1999**, *398*, 792−794.
(45) Nakade, S.; Kambe, S.; Kitamura, T.; Wada, Y.; Yanagida, S. *J. Phys. Chem. B* **2001**, *105*, 9150−9152.
(46) Kopidakis, N.; Schiff, E. A.; Park, N.-G.; Van de Lagemaat, J.; Frank, A. J. *J. Phys. Chem. B* **2000**, *104*, 3930−3936.
(47) Kambe, S.; Nakade, S.; Kitamura, T.; Wada, Y.; Yanagida, S. *J. Phys. Chem. B* **2002**, *106*, 2967−2972.
(48) Nakade, S.; Kanzaki, T.; Kubo, W.; Kitamura, T.; Wada, Y.; Yanagida, S. *J. Phys. Chem. B* **2005**, *109*, 3480−3487.
(49) Halme, J.; Vahermaa, P.; Miettunen, K.; Lund, P. *Adv. Mater.* **2010**, *22*, E210−E234.